Kinetic percolation

W. R. Heinson, A. Chakrabarti, and C. M. Sorensen

Phys. Rev. E **95**, 052109 — Published 5 May 2017

DOI: 10.1103/PhysRevE.95.052109

Kinetic Percolation

W. R. Heinson,[1] A. Chakrabarti[2] and C. M. Sorensen[2,*]

[1]*Department of Energy, Environmental & Chemical Engineering, Washington University, St. Louis, Missouri 63130, USA*

[2]*Department of Physics, Kansas State University, Manhattan, Kansas 66506, USA*

Abstract.

We demonstrate that kinetic aggregation forms superaggregates that have structures identical to static percolation aggregates, and these superaggregates appear as a separate phase in the size distribution. Diffusion limited cluster-cluster aggregation (DLCA) simulations were performed to yield fractal aggregates with a fractal dimension of 1.8 and superaggregates with a fractal dimension of $D = 2.5$ composed of these DLCA supermonomers. When properly normalized to account for the DLCA fractal nature of their supermonomers, these superaggregates have the exact same monomer packing fraction, scaling law prefactor, and scaling law exponent (the fractal dimension) as percolation aggregates; these are necessary and sufficient conditions for same structure. The size distribution remains mono-modal until these superaggregates form to alter the distribution. Thus the static percolation and the kinetic descriptions of gelation are now unified.

I. INTRODUCTION

Aggregation is a simple process in which particles in a sol, an aerosol or colloid, come together and stick to form larger particles. If the particles do not coalesce but keep their original shape (nearly) when they stick, this simple process yields a remarkable structure for the aggregates: a scale invariant, fractal structure with a quantifiable scaling dimension, the fractal dimension, D, which is less than the spatial dimension, d. Furthermore, if the system is left undisturbed for a long enough time, another marvel occurs: the sol becomes a volume filling solid structure, a gel. The primary reason that the gel forms is because with $D < d$, the growing aggregates consume the available space until none is left. Then the connectivity length scale diverges and a gel of "infinite" extent is formed. This is the kinetic description of the sol-gel transition [1-4].

Another successful description of gelation is the percolation model[5-7].One version of this model fills the available space with a point lattice. Then spherical monomers with diameter equal to the lattice spacing are placed, one by one, randomly on the lattice. Monomers occupying adjacent points touch hence are joined and become part of the same aggregate. It is found that at some critical concentration p_c, an infinite, space filling aggregate with a fractal dimension of $D =$

2.5 is created; this is the gel. Given that the monomers are placed on the lattice without regard to any time scale, the percolation model is a static model and hence does not describe the kinetics from sol to gel. Nevertheless, it successfully describes many critical-phenomena-like, power law divergences of various physical properties as the concentration of monomers p approaches the critical concentration. These results imply that the structure of a gel is that of a percolation aggregate with $D = 2.5$, not that of, for example, a diffusion limited cluster-cluster aggregation (DLCA) aggregate formed kinetically with $D = 1.8$.

Both the kinetic and percolation models gel with the emergence of a small fraction of giant clusters separate from the growing distribution of clusters present before gelation. Although this phase-transition-like behavior can result from the kinetics of simple binary collisions [8, 9], it has been rigorously connected to a thermodynamic functional [10]. A complete description of gelation would incorporate the relevant aspects of both descriptions. Can the kinetic model, which successfully describes the sol's approach to the gel, yield percolation aggregates which successfully describes critical phenomena near the gel point and will these aggregates be a distinct phase in the size distribution?

Our work with soot aerosols has extended the viability of the kinetic description of the sol-gel transition[11-16]. Experiments involving both light scattering and electron microscope studies of soot aerosol aggregation in the late stages of aggregate growth explicitly demonstrated superaggregates with a fractal dimension of $D = 2.5$, the same as the percolation value. The term "superaggregate" was coined because superaggregates are hybrids composed of smaller aggregates with a different, $D = 1.8$ fractal morphology. Simulations[12, 14] support these results and conclude that superaggregates form via DLCA which passes from aggregate dilute regime (when the mean aggregate size is much less than the mean aggregate nearest neighbor separation), where the $D = 1.8$ aggregates are formed, to the aggregate dense regime (size comparable to separation) leading to gelation. When the volume fraction of the DLCA aggregates is unity, the system is at the *ideal gel point* and the DLCA aggregates, assumed to be monodisperse and spherically shaped (hence the qualification "ideal"), obtain a size, the radius of gyration at the ideal gel point $R_{g,G}$, given by[1, 14]

$$R_{g,G} = a\left[\frac{k_0}{f_v}\left(\frac{D}{D+2}\right)^{\frac{3}{2}}\right]^{\frac{1}{3-D}} \qquad (1)$$

In Eq. (1) a is the monomer radius (assumed spherical), k_0 is the scaling prefactor, described below in Eq. (2) and f_v is the monomer volume fraction. Equation (1) is consistent with earlier studies [2, 17] that indicated that the kinetic and percolation approaches can merge at the "critical growth stage" that occurs late in the aggregation process were the aggregate volume fraction approaches unity. There the aggregates become "huge monomers" with size $R_{g,G}$ that percolate to form the gel.

What appears to be missing from a complete kinetic description of the sol-gel transition is to show that the kinetics can yield aggregates that are structurally (morphologically) *identical* to

percolation aggregates. Indeed, the equivalent fractal dimension of $D = 2.5$ for both the static percolation aggregate and the kinetically grown superaggregate is very suggestive of structural equivalence, but by no means conclusive. This begs the question: how does one determine structural identity for fractal aggregates? We have answered that question by showing there is a three parameter description that completely specifies the structure[18]. Two of the parameters, the fractal dimension D and a prefactor k_0 [19], which is related to shape[20], appear in the scaling relation for the aggregate:

$$N = k_0(R_g/a)^D \quad (2)$$

In Eq. (2) N is the number of monomers per aggregate (the monomer count), R_g is the radius of gyration of the aggregate, and a is the radius of the monomer. The third parameter is the monomer packing fraction, φ, within the aggregate. Thus if aggregates created by two different schemes have the same D, k_0 and φ, they are structurally equivalent.

In this work we show that the canonical DLCA algorithm yields superaggregates with fractal dimension, prefactor and monomer packing fraction identical to static bond percolation aggregates. The "monomers" of the superaggregates are DLCA aggregates with $D = 1.8$ that make up the superaggregate. This percolated superaggregate occurs for a large range of monomer volume fractions.

II. METHODS

Static percolation aggregates were created by placing spherical monomers with radius a randomly on a three dimensional cubic lattice until the system reached the percolation concentration p_c. For a three dimensional cubic lattice p_c=0.3116[21, 22]. It has been shown that a cubic lattice has a nearly identical percolation threshold and aggregate morphology to that of randomly packed spheres in continuous three dimensional space[23]. The simulation box size was set to various sizes to create different size aggregates.

The kinetically formed aggregates were created using an off-lattice, DLCA algorithm[20, 24]. Initially 10^7 spherical monomers were randomly placed into a three dimensional simulation box. The monomer volume fraction, f_v was controlled by the box size. As DLCA starts, the number of aggregates N_c including lone monomers is counted. An aggregate is randomly chosen and simulation time is incremented by N_c^{-1}. The probability that an aggregate moves is inversely proportional to the aggregate's radius of gyration and is normalized to insure the monomers will always move upon selection. If the aggregate moves, it travels randomly one monomer diameter $2a$. When two aggregates collide, they irreversibly stick and N_c is decremented by 1. Results are applicable in the continuum limit where the frictional drag is given by the Stokes–Einstein expression with a drag proportional to the radius of gyration.

III. RESULTS

Figure 1 shows the number of monomers N in a kinetic aggregate versus aggregate R_g normalized by monomer radius a on a log-log plot for initial monomer volume fractions of f_v = 0.003, 0.01, 0.02, 0.1. This is a test of Eq. (2) for these aggregates. The trend of the data starts as the canonical DLCA with D = 1.8 and k_0 = 1.35, but at large sizes, the aggregates transition to D = 2.5. This demonstrates the crossover from normal DLCA aggregates with D = 1.8 and k_0 = 1.35 to superaggregates with D = 2.5 as found before. The empirical transition size from D = 1.8 to D = 2.5 is in agreement with that calculated by Eq. (1).

The simple average size $<R_0>$ of the normal DLCA aggregates is marked for each ensemble plot in Fig.1. We propose that $<R_0>$ represents the average size of the normal DLCA aggregates that comprise the monomers of the superaggregate. Thus we call these normal DLCA aggregates "supermonomers". These supermonomers follow the trend of Eq. (2) with k_o = 1.35 and D = 1.8 that has been reported before for DLCA systems[18, 19, 25].

Figure 1 also shows that after several DLCA supermonomers come together to form a superaggregate with $R_g > R_{g,G}$, they follow the trend of Eq. (2) with D = 2.5, but the prefactor k_0 depends on where the $R_{g,G}$ crossover happens, which in turn is controlled by the initial monomer volume fraction as described in Eq. (1). These values are marked in Fig. 1. Small f_v leads to small k_0 for the superaggregates.

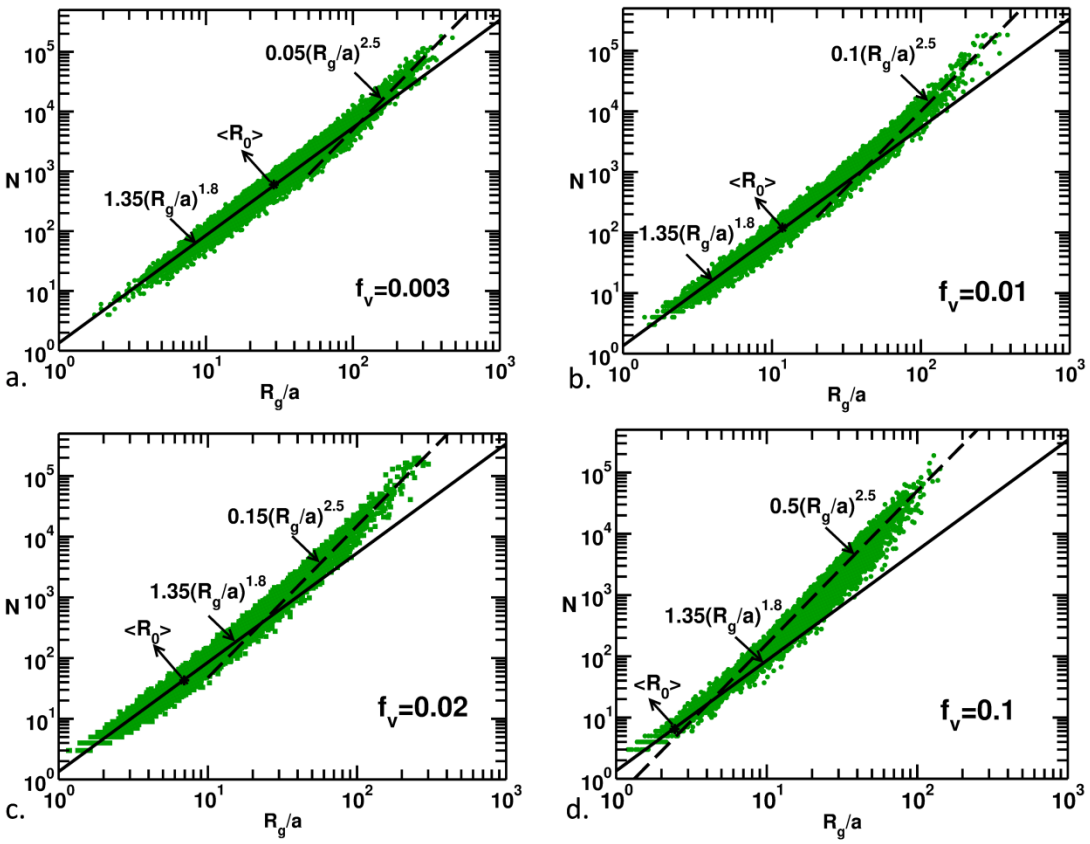

Figure 1. Aggregate monomer count N versus aggregate radius of gyration R_g normalized by monomer radius a on log-log plots. Linear regimes imply the power law as described in Eq. (2), the slope is the exponent, the fractal dimension D. All systems start at small R_g/a with D = 1.8 and a prefactor k_0 = 1.35. In (a) the initial monomer fraction was f_v = 0.003 and the system reached a D = 2.5 with a prefactor of k_0 = 0.05 regime at large R_g/a. In (b) f_v = 0.01 and reached D = 2.5 with k_0 = 0.10. In (c) f_v = 0.02 and reached D = 2.5 with k_0 =0.15. In (d) f_v = 0.1 and reached D = 2.5 with k_0 = 0.50. In all plots the average supermonomer size $<R_0>$ is marked.

The same data appear in Fig. 2a, however, here the R_g is broken into equal sized bins and for each R_g bin the average N is calculated. This binning was done for clarity; it allows the plots for the different f_v to be resolved from each other. In Fig. 2b R_g is normalized by the average supermonomer radius $<R_0>$and plotted against N normalized by average supermonomer number count $<N_0>$. Under the normalization with $<R_0>$ and $<N_0>$, a universal trend becomes apparent as the superaggregates, regardless of the monomer volume fraction f_v, follow the percolation aggregates' trend quantified by k_0 = 0.6 and D = 2.5 for each. Note that the data in Fig. 2a indicate that the aggregates must contain at least ten to thirty constituent particles before they can differentiate themselves. Thus we find that the percolation result and the supermonomer normalized kinetic results are identical.

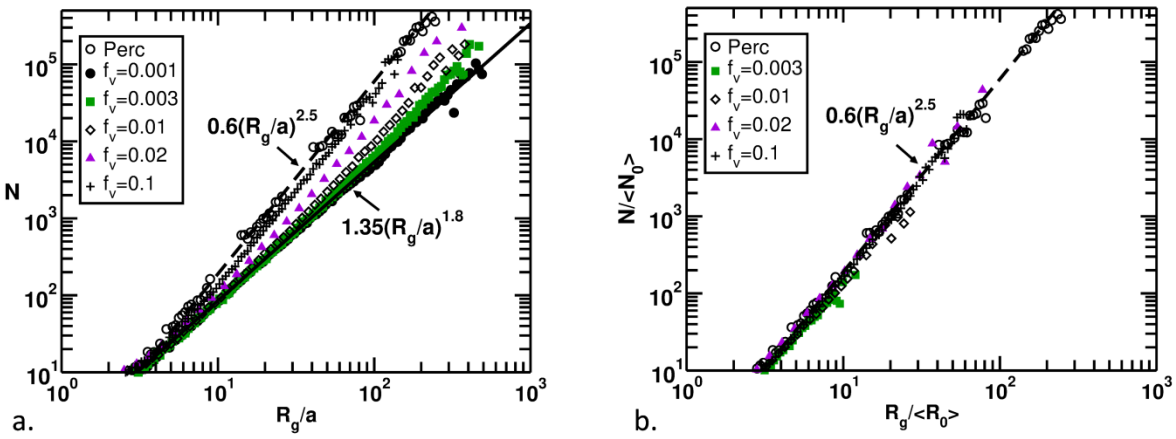

Figure 2. In (a) R_g data from Fig. 1 is binned and the average N for each bin is plotted for clarity. The data in (a) indicates that small aggregates i.e. N <10-30, cannot differentiate themselves between D = 1.8 and D =2.5. In (b) the R_g values from (a) are normalized by the supermonomer radius $\langle R_0 \rangle$, and N is normalized by the supermonomer count $\langle N_0 \rangle$. These renormalized plots now all fall onto a single trend. Furthermore, the trend overlaps that for aggregates made via the simple, cubic lattice, static percolation algorithm. The fit to Eq. (2) for all these yields D = 2.5 and k_0 = 0.6.

In 3d space the number of monomers in a volume with radius r is $N(r) = \varphi\,(r/a)^3$ where φ is the packing fraction. For fractal aggregates this generalizes to[18, 26]

$$N(r) = \varphi(r/a)^D \tag{3}$$

The monomer pair correlation function $g(r)$ is the probability that another monomer will be present a distance r from a given monomer. Thus for aggregates, $g(r)$ is proportional to the average number of monomers in a shell of radius r and thickness dr.

$$g(r) \propto \left\langle \frac{monomers\ in\ dV}{4\pi r^2 dr} \right\rangle \tag{4}$$

With Eqs. (3) and (4), the pair-correlation becomes

$$g(r) = \frac{dN}{4\pi r^2 dr} = \frac{D\varphi}{4\pi a^D} r^{D-3} \tag{5}$$

For an isotropic aggregate the correlation function is constrained by the normalization condition that the volume integral of $g(r)$ equals N. To achieve this normalization for Eq. (5) the finite size of an aggregate must be accounted for. Therefore a cutoff function is added. It is customary to use a stretched exponential function as the cutoff function. Thus

$$g(r) = \frac{D\varphi}{4\pi a^D} r^{D-3} exp[-(r/\xi)^\gamma] \tag{6}$$

where the stretching exponent γ has been shown to be an indicator of a aggregate's shape anisotropy[18, 20].

In Fig. 3 the pair correlation functions *g(r)* for pure DLCA (volume fraction $f_v = 0.001$), DLCA leading to superaggregates, and a percolation aggregate are shown. We apply the same approach used in[18]. In Figs. 3a and 3f the fits to Eq. (6) for the monomer packing φ and power law exponent $D - 3$ are shown for a pure DLCA aggregate and a static percolation aggregate, respectively. The fit for the pure DLCA aggregates follow the power law corresponding to $D = 1.8$, consistent with the results from Figs. 1 and 2, and packing fraction $\varphi = 0.7$[18]. The fit for the percolation aggregates exhibit a power law corresponding to $D = 2.5$ and monomer packing fraction $\varphi = 0.3$, which is the canonical results for these types of aggregates[27].

The superaggregates in Figs. 3b-e were generated kinetically as described above with $f_v = 0.003$, 0.01, 0.02, 0.1 and have *g(r)* in concordance with Eq. (6) with power laws and monomer packing fractions that agree with DLCA at small *r* until a crossover begins at about $<R_0>$. Then at $R_{g,G} > <R_0>$ the trend in *g(r)* for larger *r* follows a power law that corresponds to $D = 2.5$.

A pair-correlation function of supermonomers g_G can be found by replacing monomer radius *a* with $<R_0>$ and using the normalization condition

$$\int g_G(r) 4\pi r^2 dr = \frac{N}{\langle N_0 \rangle} \tag{7}$$

This leads to

$$g_G(r) = \frac{D\varphi_0}{4\pi \langle R_0 \rangle^D} r^{D-3} \exp\left[-(r/\xi)^\gamma\right] \tag{8}$$

From Eq. (8) it is possible to find the supermonomer packing fraction represented by φ_0. The supermonomer packing fraction for monomer volume fractions $f_v = 0.003$, 0.01, 0.02 and 0.1 were all found to be $\varphi_0 = 0.3$ in agreement with the monomer packing fraction of the static percolation aggregates, suggesting that superaggregates are percolation aggregates with DLCA aggregates as supermonomers.

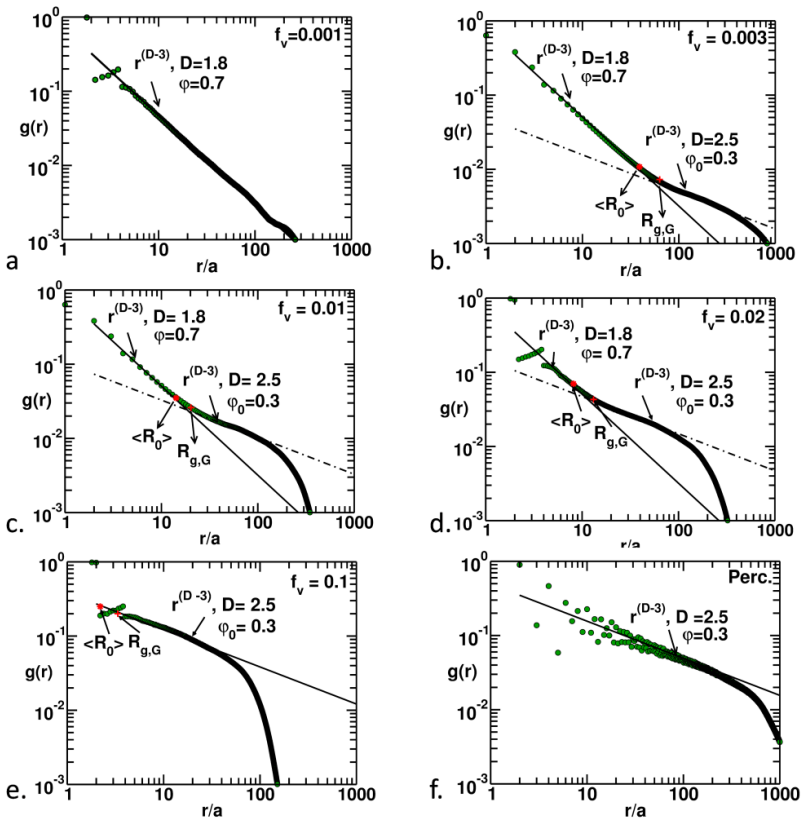

Figure 3. The pair correlation function *g(r)* for aggregates (circles symbols) taken from DLCA simulations with fits lines derived from Eq. (6) and (8). The monomer packing fraction φ = 0.7 is found for all DLCA aggregates below the superaggregate crossover between $<R_0>$ and $R_{g,G}$. In (a) an aggregate taken from a DLCA system with f_v = 0.001 that has not developed into superaggregates. For (b) to (e), *g(r)* of aggregates with f_v = 0.003, 0.01, 0.02 and 0.1, respectively, the average supermonomer size $<R_0>$ and radius of gyration at the gel point $R_{g,G}$ are marked. The crossover from D = 1.8 to D = 2.5 is flanked by $<R_0>$ on the left and $R_{g,G}$ on the right at larger r. In (f) the *g(r)* of a static percolation aggregate is plotted and is described by φ_0 = 0.3 and D = 2.5 which matches the DLCA superaggregates well.

The equality of the three parameters D, k_0 and φ between the percolation aggregate and the monomer renormalized superaggregates demonstrates that the kinetically formed superaggregates have structures identical to the static percolation aggregates.

Finally, Fig. 4 shows the size distribution behavior for the two intermediate monomer volume fractions f_v = 0.01 and 0.02. The aggregation proceeds as indicated by the total number of clusters, N_c, decreasing. For large N_c, hence early times, the distributions are mono-modal. However, bi-modality is seen at later stages with the advent of large clusters. The number of these clusters is small as seen in the particle count spectra, while the fraction of mass in the larger size mode is significant as seen in the particle mass spectra. This is the well-known, phase-transition-like behavior that occurs when a sol becomes a gel, i.e. at gelation[8-10]. This few in

number, large in mass population are the superaggregates with their hybrid morphology displayed in Figs. 1, 2 and 3, above.

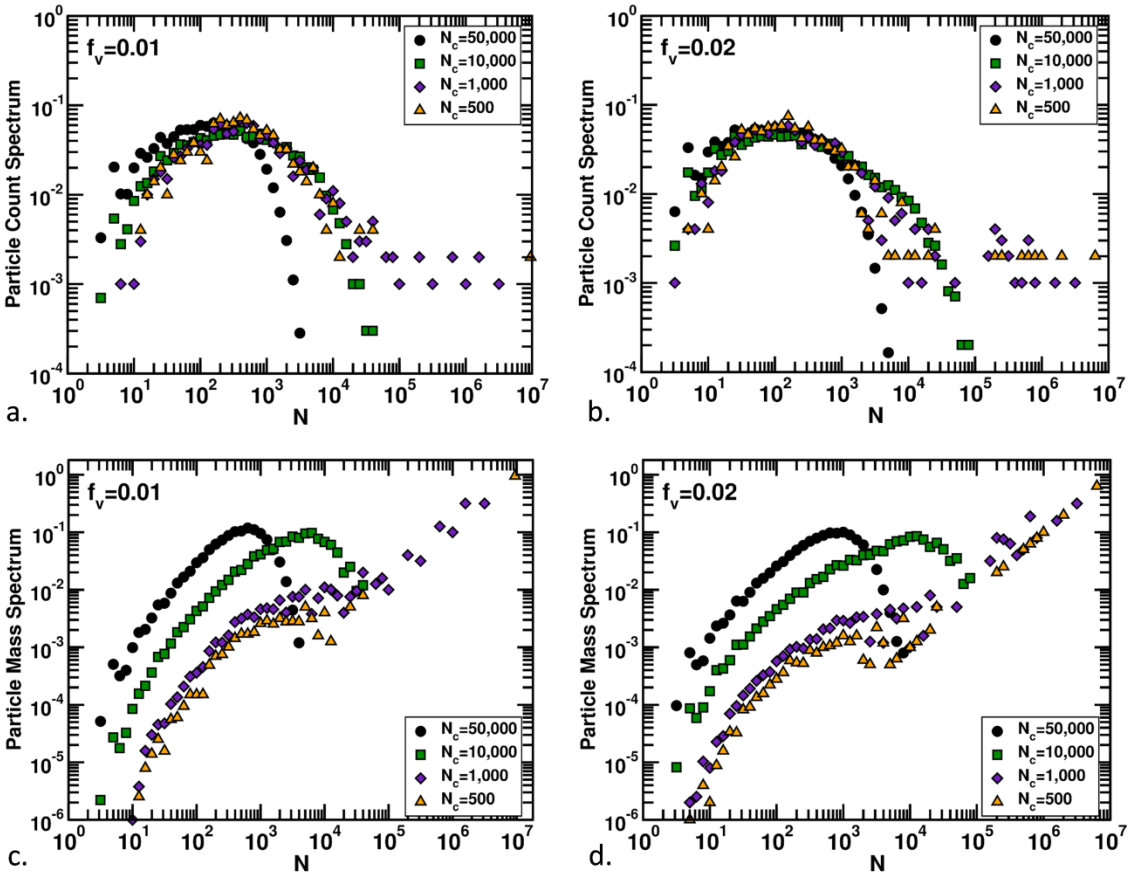

Figure 4. Particle count spectra (upper plots) and particle mass spectra (lower plots) for two monomer volume fractions f_v = 0.01 and 0.02. N_c is the total number of clusters remaining in the aggregation run.

IV. CONCLUSIONS

In summary, with these results, one complete description of gelation that incorporates the relevant aspects of both the kinetic and percolation descriptions is provided: Diffusion limited cluster aggregation (DLCA) produces fractal aggregates with a fractal (scaling) dimension of 1.8; these are DLCA aggregates, a well-known result. Because this scaling dimension is less than the spatial dimension, continued aggregate growth ultimately leads to a DLCA aggregate volume fraction of unity; this is the ideal gel point. Kinetic aggregation near this point leads to superaggregates with a fractal dimension of $D = 2.5$ composed of DLCA supermonomers. These superaggregates, when properly normalized to account for the DLCA fractal nature of their supermonomers, have the exact same structure as static percolation aggregates as specified by

the monomer packing fraction, scaling law prefactor, and scaling law exponent. Furthermore, they comprise a distinct population, few in number but large in mass, of the aggregate size distribution which is not present before gelation. Thus the kinetics provides one complete conceptual framework for gelation. There is no need to artificially add a static percolation aggregate at the end of a kinetic growth period; percolation is a natural result of kinetic growth. These two descriptions of gelation are now joined.

It is reasonable to expect that any other cluster-cluster aggregation mechanism, such as reaction limited cluster-cluster aggregation (RLCA), that yields a fractal dimension less than the spatial dimension will also yield superaggregates with the same percolation aggregate structure but with different, "supermonomer" fractal dimension.

ACKNOWLEDGMENTS

This work was supported by the National Science Foundation, Directorate for Geosciences (GEO) (AGM 1261651), National Science Foundation (NSF) (AGS1455215, CBET-1511964, AGS-PRF1624814) and NASA Radiation Sciences Program (NNX15AI66G).

*Corresponding author: sor@phys.ksu.edu

References.

1. C. M. Sorensen and A. Chakrabarti, Soft Matter **7** (6), 2284-2296 (2011).
2. J. E. Martin and D. Adolf, Annu Rev Phys Chem **42**, 311-339 (1991).
3. W. C. K. Poon and M. D. Haw, Adv Colloid Interfac **73**, 71-126 (1997).
4. E. Zaccarelli, J Phys-Condens Mat **19** (32), 323101 (2007).
5. D. Stauffer, J Chem Soc Farad T 2 **72**, 1354-1364 (1976).
6. P. G. Degennes, J Phys Lett-Paris **37** (1), L1-L2 (1976).
7. D. Stauffer, A. Coniglio and M. Adam, Adv Polym Sci **44**, 103-158 (1982).
8. A. A. Lushnikov, Phys Rev Lett **93** (19) (2004).
9. A. A. Lushnikov, Phys Rev E **71** (4), 046129 (2005).
10. T. Matsoukas, Sci Rep-Uk **5** (2015).
11. C. M. Sorensen, B. Hageman, T. J. Rush, H. Huang and C. Oh, Phys Rev Lett **80** (8), 1782-1785 (1998).
12. C. M. Sorensen, W. Kim, D. Fry, D. Shi and A. Chakrabarti, Langmuir **19** (18), 7560-7563 (2003).
13. W. Kim, C. M. Sorensen and A. Chakrabarti, Langmuir **20** (10), 3969-3973 (2004).
14. D. Fry, A. Chakrabarti, W. Kim and C. M. Sorensen, Phys Rev E **69** (6) (2004).
15. R. Dhaubhadel, F. Pierce, A. Chakrabarti and C. M. Sorensen, Phys Rev E **73** (1) (2006).
16. W. G. Kim, C. M. Sorensen and A. Chakrabarti, J. Aerosol Science **37**, 386- 401 (2006).
17. J. E. Martin and J. P. Wilcoxon, Phys Rev A **39** (1), 252-258 (1989).
18. W. R. Heinson, C. M. Sorensen and A. Chakrabarti, J Colloid Interf Sci **375**, 65-69 (2012).
19. C. M. Sorensen and G. C. Roberts, J Colloid Interf Sci **186** (2), 447-452 (1997).
20. W. R. Heinson, C. M. Sorensen and A. Chakrabarti, Aerosol Science and Technology **44** (12), i-iv (2010).

21. M. Acharyya and D. Stauffer, Int J Mod Phys C **9** (4), 643-647 (1998).
22. X. Xu, J. F. Wang, J. P. Lv and Y. J. Deng, Front Phys-Beijing **9** (1), 113-119 (2014).
23. M. J. Powell, Phys Rev B **20** (10), 4194-4198 (1979).
24. P. Meakin, J Colloid Interf Sci **102** (2), 505-512 (1984).
25. P. Meakin, Adv Colloid Interfac **28** (4), 249-331 (1988).
26. T. Nicolai, D. Durand and J. C. Gimel, Phys Rev B **50** (22), 16357-16363 (1994).
27. D. Stauffer and A. Aharony, *Introduction to Percolation Theory: Revised Second Edition*. (Taylor & Francis, New York, 1994).